

INTRODUCTION

The precise automatic segmentation of brain tissues such as white matter (WM), gray matter (GM) and cerebrospinal fluid (CSF) of MRI is of great importance for accurate evaluation of early brain development.

(1) Convolutional neural networks (CNNs) have been used for brain tissue segmentation:

- 2D U-Net: Ronneberger et al. (Ref. [1])
- V-Net: Milletari et al. (Ref. [2])
- 3D U-Net: (Ref. [3])
- VoxResNet: Chen et al. (Ref. [4])

(2) Attention mechanism has been used in medical image segmentation:

- Binary version of sSE: Roy et al. (Ref. [5])
- A novel attention gate (AG): Oktay et al. (Ref. [6])
- A connection sensitive attention U-Net (CSAU): Li et al. (Ref. [7])

Contributions:

- (1) a novel Binary Channel Attention Module (BCAM) to better provide more precise anatomical segmentation.
- (2) Spatial pyramid pooling (SPP) [8] modules with different pooling operations are used in BCAM to better aggregate multi-scale spatial information of the feature map.

METHODS

1. Attention Module

Squeeze-and-Excitation (SE), Spatial Squeeze and Channel Excitation (cSE), Channel Squeeze and Spatial Excitation (sSE), Mixed-Supervised Dual-Network (MSDN), Convolutional Block Attention Module (CBAM)

2. Binary Channel Attention Module (BCAM)

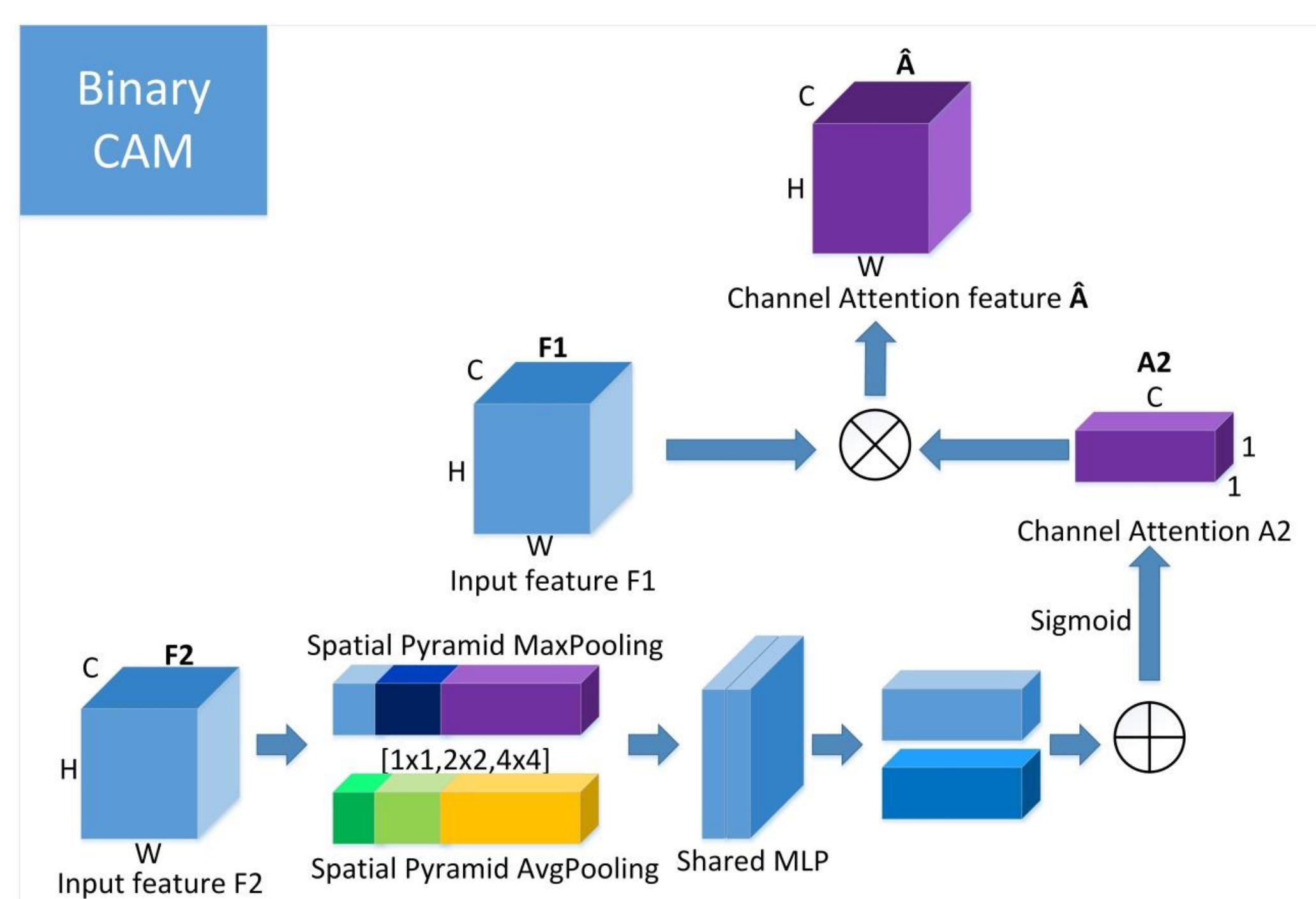


Fig. 1. Binary Channel Attention Module (BCAM)

- Spatial Pyramid average-Pooling (SPP with average-pooling)
- Spatial Pyramid max-Pooling (SPP with max-pooling)
- instead of average-pooling and max-pooling operations: to better aggregate multi-scale spatial information of the feature map (3-level pyramid average-pooling and max-pooling (1x1, 2x2, 4x4) with total 21 bins respectively)
- the channel attention is computed as:

$$\text{Eq. (1)} \quad A2(F2) =$$

$$\sigma \left(MLP(SP_{Avg} Pooling(F2)) + MLP(SP_{Max} Pooling(F2)) \right)$$

$$\sigma \left(W_1(W_0(F_{Spp-avg}^c)) + W_1(W_0(F_{Spp-max}^c)) \right)$$

$$\text{Eq. (2)} \quad \hat{A} = A2(F2) \otimes F1$$

3. Network Structure

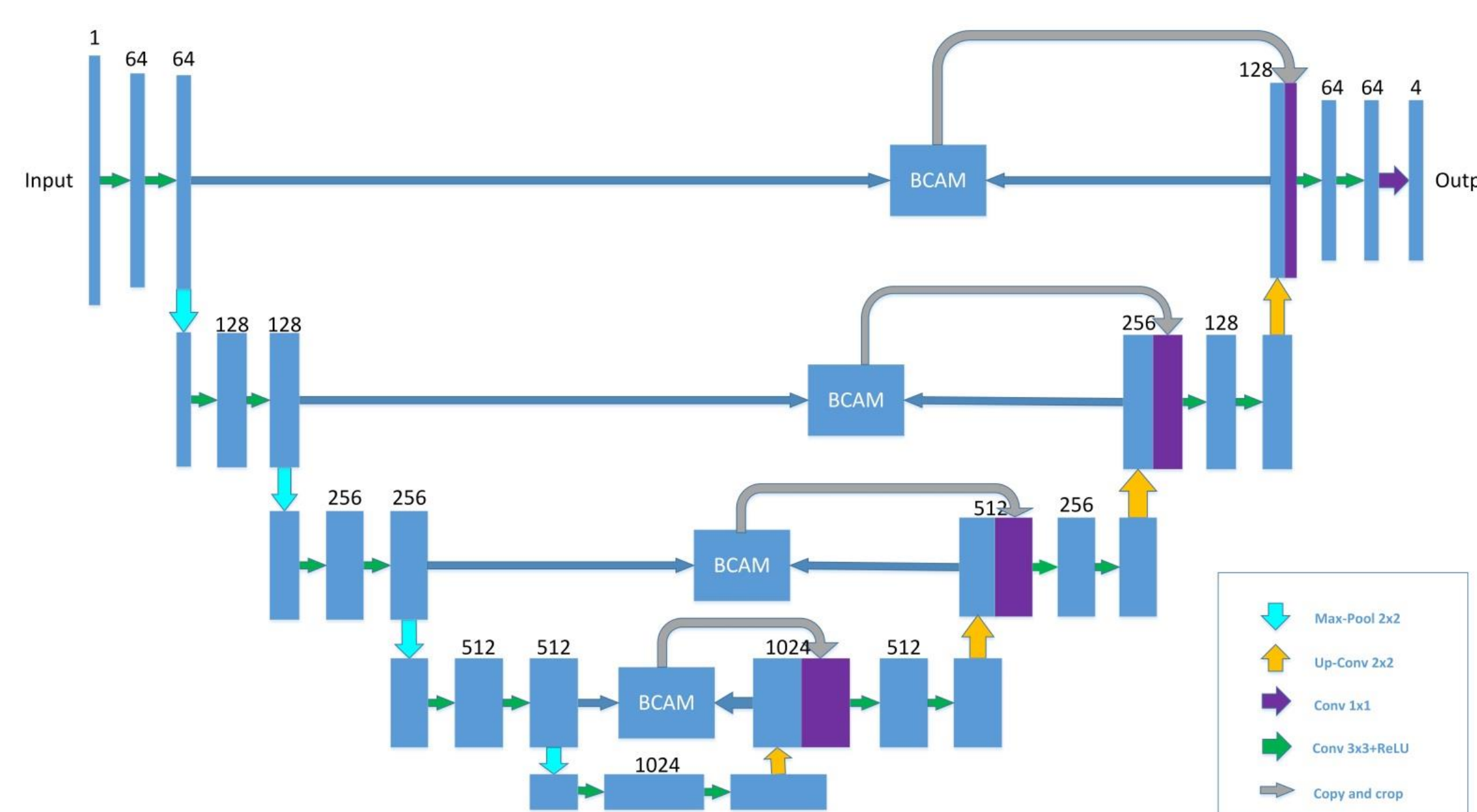


Fig. 2. BCAU-Net architecture.

- The BCAM modules are added into the skip-connection between each encoder stage and corresponding decoder stage.
- The feature map from the output of each BCAM is concatenated with the corresponding feature map that after up-sampling in the decoder stage, utilizing the inter-channel relationship of corresponding low-level feature (low-resolution information after maxpooling) and high-level feature (high-resolution information after up-sampling).

RESULTS

1. Datasets

IBSR: 18 MRI volumes (01-18 scans, size: 256 × 128 × 256) and the corresponding ground truth (GT)

MRBrainS18: including T1-weighted, T1-IR and T2-FLAIR, seven brain MRI scans (1,4,5,7,14,070,148, size: 240 × 240 × 48) with manual segmentations are provided.

2. Evaluation Criteria

Dice coefficient [9] (DC) (higher is better), the 95th-percentile of Hausdorff distance (HD) (lower is better) and absolute volume difference (AVD) (lower is better)

3. Implementation Details

GeForce GTX 1080 Ti GPU, Keras

5-fold cross-validation

• Loss function:

$$\text{Eq. (3)} \quad L = L_{Dice} + \alpha L_{CE}$$

$$L = L_{Dice} + \alpha L_{CE}$$

$$\text{Eq. (4)} \quad L_{Dice} = 4 - \sum_{i=0}^3 \frac{2 \sum_{i=0}^N p_i y_i + \epsilon}{\sum_{i=0}^N p_i + \sum_{i=0}^N y_i + \epsilon}$$

$$\text{Eq. (5)} \quad L_{CE} = -\frac{1}{N} \left(\sum_{i=0}^N p_i y_i + \sum_{i=0}^N (1-p_i)(1-y_i) \right)$$

$$L_{CE} = -\frac{1}{N} \left(\sum_{i=0}^N p_i y_i + \sum_{i=0}^N (1-p_i)(1-y_i) \right)$$

4. Experimental Results

TABLE I
RESULTS OF 5-FOLD CROSS VALIDATION ON IBSR DATASET FOR DIFFERENT EXPERIMENTS (DC: %, HD: MM, AVD: %). THE BEST OBTAINED RESULTS ARE PRESENTED IN THE FIVE FOLDS FOR IBSR. BEST RESULTS ARE HIGHEST IN BOLD.

Experiment	DC			Avg. DC	HD			Avg. HD	AVD			Avg. AVD
	CSF	GM	WM		CSF	GM	WM		CSF	GM	WM	
2D U-Net (Baseline) [6]	85.19	90.34	89.20	88.24	3.0835	1.9665	2.4675	2.5058	8.52	1.68	5.21	5.14
3D U-Net [13]	85.51	89.58	89.33	88.48	3.0494	1.7711	1.8949	2.5425	9.90	1.72	5.26	4.56
VoxResNet [4]	71.58	91.37	90.23	84.39	19.1106	1.5159	1.7693	7.4653	18.77	3.84	4.61	9.07
BCAU-Net-R	83.34	91.04	89.77	88.05	3.3411	1.8781	2.2081	2.4758	10.10	1.21	4.00	5.10
BCAU-Net	85.41	91.38	89.78	88.86	2.9370	1.8744	2.0858	2.2991	7.72	0.97	2.83	3.84
BCAU-Net-E	84.18	91.02	89.69	88.30	3.3655	1.8715	2.1059	2.4476	9.43	1.37	4.38	5.06

- RCAU-Net produces better results (DC: 88.86%, HD: 2.2991mm, AVD: 3.84%) on IBSR dataset than 2D U-Net (Baseline), with a relative improvement of 0.62% on DC, which shows the effectiveness of BCAM block (TABLE I).
- BCAU-Net has the highest average DC, the lowest maximum value of HD, AVD (Fig. 3) and the best segmentation results (Fig. 4).
- It help utilize the inter-channel relationship of corresponding low-level and high-level information to better provide more precise anatomical segmentation.

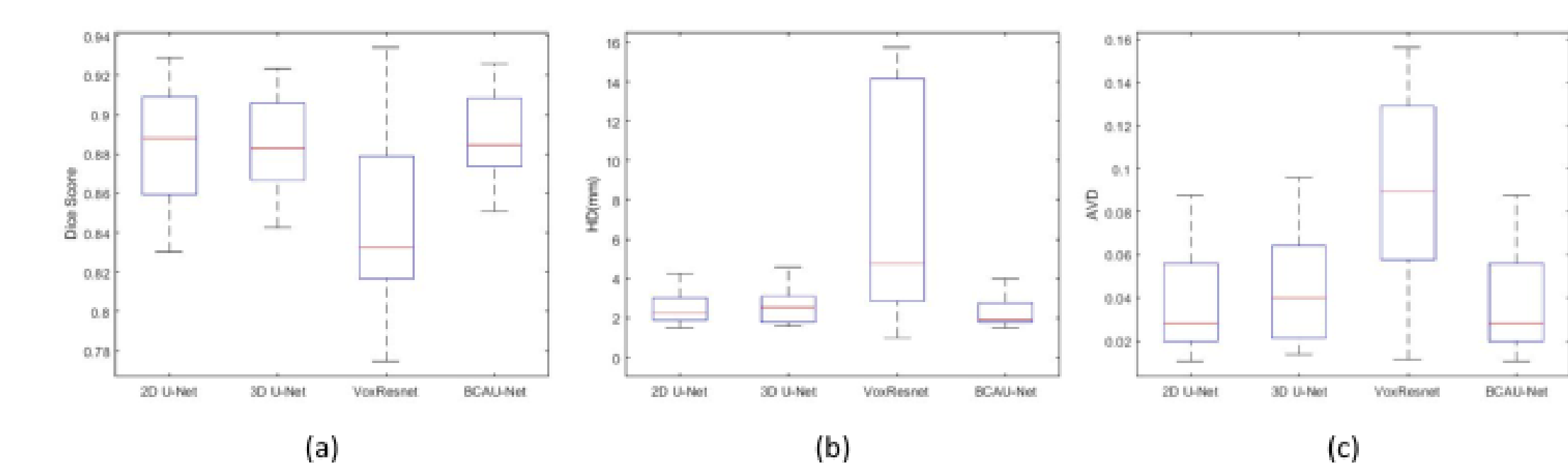


Fig. 3. Boxplots of best obtained results for different models on IBSR: (a) DC, (b) HD, (c) AVD.

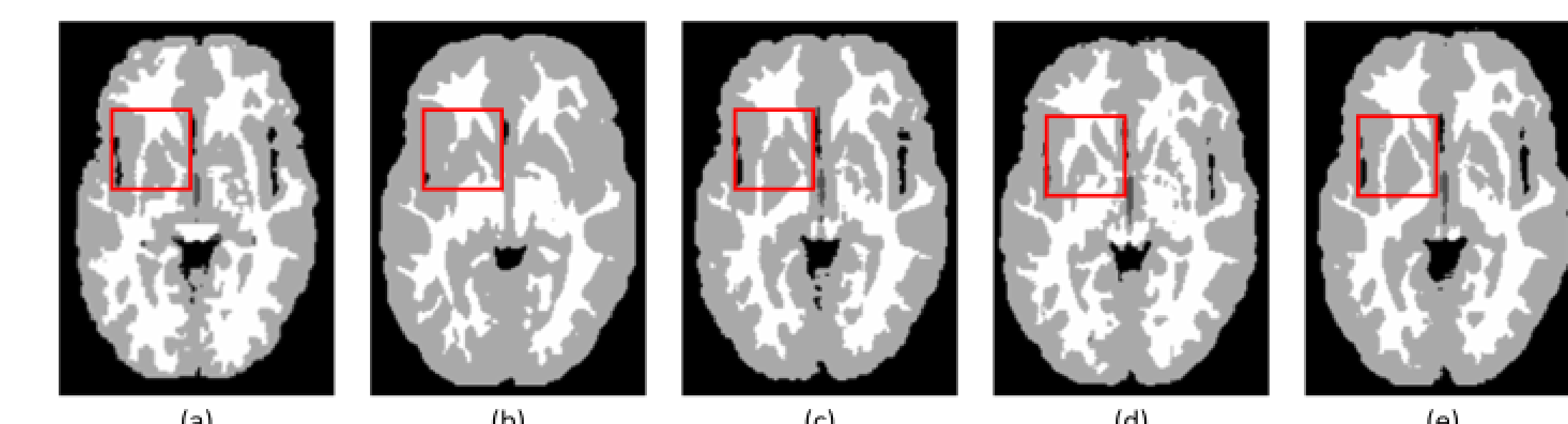


Fig. 4. Best predicted results for different models on IBSR: (a) Label (Ground Truth), (b) 2D U-Net, (c) 3D U-Net, (d) VoxResNet, (e) Our model (BCAU-Net).

CONCLUSIONS

1. Proposed a new architecture RCAU-Net by introducing a novel Binary Channel Attention Module (BCAM) into skip connection of U-Net.
2. To better aggregate multi-scale spatial information of the feature map, spatial pyramid pooling (SPP) with three pooling windows (1x1, 2x2, 4x4) are used in BCAM.
3. We verify this model on two datasets including IBSR and MRBrainS18, and obtain better performance on MRI brain segmentation compared with other methods.

REFERENCES

- [1] O. Ronneberger, P. Fischer, and T. Brox, "U-Net: Convolutional Networks for Biomedical Image Segmentation," in Medical Image Computing and Computer-Assisted Intervention, 2015, pp. 234–241.
- [2] F. Milletari, N. Navab, and S. A. Ahmadi, V-Net: fully convolutional neural networks for volumetric medical image segmentation. In Proceedings of 3DV, 2016, pp. 565–571.
- [3] O. C. İc, ek, A. Abdulkadir, S. S. Lienkamp, T. Brox, and O. Ronneberger, "3D U-Net: Learning Dense Volumetric Segmentation from Sparse Annotation," in Medical Image Computing and Computer-Assisted Intervention, 2016, pp. 424–432.
- [4] H. Chen, Q. Dou, L. Yu, J. Qin, and P. A. Heng, "VoxResNet: Deep voxelwise residual networks for brain segmentation from 3D MR images," NeuroImage, vol. 170, pp. 446–455, 2018.
- [5] A. G. Roy, S. Siddiqui, S. P. O'esterl, N. Navab, and C. Wachinger, "Squeeze and Excite' Guided Few-Shot Segmentation of Volumetric Images, unpublished.
- [6] O. Oktay, et al., Attention U-Net: Learning Where to Look for the Pancreas. In MIDL, 2018.
- [7] R. R. Li, M. M. Li, J. C. Li, and Y. T. Zhou, Connection Sensitive Attention U-NET for Accurate Retinal Vessel Segmentation, unpublished.
- [8] K. He, X. Zhang, S. Ren, and J. Sun. Spatial pyramid pooling in deep convolutional networks for visual recognition. In ECCV, 2014.
- [9] A. A. Taha and A. Hanbury, Metrics for evaluating 3d medical image segmentation: analysis, selection, and tool. BMC Medical Imaging, vol.15, no.1, pp. 29, 2015.